

AD-A209 787

TECHNICAL REPORT CR-RD-PR-89-1

**FURTHER INVESTIGATION OF FLOW MODELING  
DURING SOLID PROPELLANT PROCESSING**

Y. S. Cha  
H. M. Domanus  
W. T. Sha  
Argonne National Laboratory  
9700 South Cass Avenue  
Argonne, IL 60439

S. L. Soo  
Department of Mechanical and Industrial Engineering  
University of Illinois-Urbana  
Urbana, Illinois 61801

**MAY 1989**

Prepared for:  
Propulsion Directorate  
Research, Development, and Engineering Center

Contract No. W-31-109-ENG-38



**U.S. ARMY MISSILE COMMAND**

*Redstone Arsenal, Alabama 35898-5000*

Approved for public release, distribution is unlimited.

**SDTICD**  
ELECTE  
JUL 07 1989

CH

#### **DISPOSITION INSTRUCTIONS**

**DESTROY THIS REPORT WHEN IT IS NO LONGER NEEDED. DO NOT  
RETURN IT TO THE ORIGINATOR.**

#### **DISCLAIMER**

**THE FINDINGS IN THIS REPORT ARE NOT TO BE CONSTRUED AS AN  
OFFICIAL DEPARTMENT OF THE ARMY POSITION UNLESS SO DESIGNATED BY OTHER AUTHORIZED DOCUMENTS.**

#### **TRADE NAMES**

**USE OF TRADE NAMES OR MANUFACTURERS IN THIS REPORT DOES  
NOT CONSTITUTE AN OFFICIAL INDORSEMENT OR APPROVAL OF  
THE USE OF SUCH COMMERCIAL HARDWARE OR SOFTWARE.**

TECHNICAL REPORT CR-RD-PR-89-1

FURTHER INVESTIGATION OF FLOW MODELING  
DURING SOLID PROPELLANT PROCESSING

by

Y. S. Cha, H. M. Domanus, W. T. Sha

Materials and Components Technology Division  
Argonne National Laboratory  
9700 South Cass Avenue  
Argonne, Illinois 60439

and

S. L. Soo

Department of Mechanical and Industrial Engineering  
University of Illinois-Urbana  
Urbana, Illinois 61801

May 1989

Approved for public release, distribution is unlimited.

Prepared for:  
Propulsion Directorate  
Research, Development, and Engineering Center

Contract No. W-31-109-ENG-38

UNCLASSIFIED

SECURITY CLASSIFICATION OF THIS PAGE

REPORT DOCUMENTATION PAGE				Form Approved OMB No 0704-0188 Exp Date Jun 30, 1986	
1a REPORT SECURITY CLASSIFICATION <u>Unclassified</u>			1b. RESTRICTIVE MARKINGS		
2a SECURITY CLASSIFICATION AUTHORITY			3. DISTRIBUTION / AVAILABILITY OF REPORT  Approved for public release, distribution is unlimited.		
2b. DECLASSIFICATION / DOWNGRADING SCHEDULE			5. MONITORING ORGANIZATION REPORT NUMBER(S)  CR-RD-PR-89-1		
4. PERFORMING ORGANIZATION REPORT NUMBER(S)			7a. NAME OF MONITORING ORGANIZATION Propulsion Directorate, Research, Development and Engineering Center		
6a. NAME OF PERFORMING ORGANIZATION Argonne National Laboratory Components Technology Div		6b. OFFICE SYMBOL (If applicable)  AMSMI-RD-PR-F		7b. ADDRESS (City, State, and ZIP Code) Commander U.S. Army Missile Command ATTN: AMSMI-RD-PR Redstone Arsenal, AL 35898-5249	
6c. ADDRESS (City, State, and ZIP Code)  9700 South Cass Avenue Argonne, IL 60439			9. PROCUREMENT INSTRUMENT IDENTIFICATION NUMBER  Contract No. W-31-109-ENG-38		
8a. NAME OF FUNDING / SPONSORING ORGANIZATION Propulsion Directorate, Res. Dev. and Eng Ctr		8b. OFFICE SYMBOL (If applicable)  AMSMI-RD-PR-F		10. SOURCE OF FUNDING NUMBERS	
8c. ADDRESS (City, State, and ZIP Code) Commander U.S. Army Missile Command ATTN: AMSMI-RD-PR Redstone Arsenal, AL 35898-5249		PROGRAM ELEMENT NO.  61101A		PROJECT NO.  IL161101A91A	
		TASK NO.		WORK UNIT ACCESSION NO.	
11. TITLE (Include Security Classification)  Further Investigation of Flow Modeling During Solid Propellant Processing (U)					
12. PERSONAL AUTHOR(S) Y. S. Cha, H. M. Domanus, W. T. Sha, S. L. Soo					
13a. TYPE OF REPORT Final		13b. TIME COVERED FROM 9/87 TO 9/88		14. DATE OF REPORT (Year, Month, Day) May 1989	
				15. PAGE COUNT 35	
16. SUPPLEMENTARY NOTATION					
17. COSATI CODES			18. SUBJECT TERMS (Continue on reverse if necessary and identify by block number)		
FIELD	GROUP	SUB-GROUP	Propellant Processing		
21	08		Flow Modeling		
			Liquid/Solid Flows		
19. ABSTRACT (Continue on reverse if necessary and identify by block number)  A two-fluid model is employed to investigate the velocity and volume fraction distributions during the solid propellant casting process. Two important dimensionless parameters, the dimensionless interfacial momentum transfer coefficient $D$ , and the viscosity ratio of the two fluids $Z$ , are identified and varied parametrically in the numerical calculations. The results show that when $D$ is small ( $< 0.05$ ), separation between the particles and binder occurred and the smaller the $D$ , the larger the degree of separation. When $D$ is large ( $> 1$ ), separation did not occur since the two fluids move like a single fluid when interfacial momentum transfer is dominating. Near the transition point between separation and no separation ( $D \approx 1$ ), an M-shaped profile was observed for the particle volume fraction distribution in an annular duct. The degree of separation is very small and the reason for the existence of such an M-shaped profile is not clearly understood.  (Continued)					
20. DISTRIBUTION / AVAILABILITY OF ABSTRACT <input checked="" type="checkbox"/> UNCLASSIFIED/UNLIMITED <input type="checkbox"/> SAME AS RPT. <input type="checkbox"/> DTIC USERS			21. ABSTRACT SECURITY CLASSIFICATION Unclassified		
22a. NAME OF RESPONSIBLE INDIVIDUAL A. R. Maykut			22b. TELEPHONE (Include Area Code) (205) 876-0075		22c. OFFICE SYMBOL AMSMI-RD-PR

Block 19. (Continued)

It is pointed out that a viscosity model recently proposed by Probstein and Sengun may be relevant to the solid propellant system. It is suggested that the next logical step is to incorporate the non-Newtonian behavior of the binder (and the fine particles) into the two-fluid model.

# TABLE OF CONTENTS

	Page
1.0 INTRODUCTION.....	1
2.0 IMPORTANT PARAMETERS.....	1
3.0 EFFECTS OF INTERFACIAL DRAG AND RELATIVE VISCOSITY.....	4
4.0 DISCUSSIONS.....	5
5.0 SUMMARY.....	7
REFERENCES.....	19



Accession For	
NTIS GRA&I	<input checked="" type="checkbox"/>
DTIC TAB	<input type="checkbox"/>
Unannounced	<input type="checkbox"/>
Justification	
By	
Distribution/	
Availability Codes	
Dist	Avail and/or Special
A-1	

## 1.0. INTRODUCTION

It was observed that a bump existed in the pressure-time curve during the burning of solid rocket propellant. The pressure bump is likely due to a concentration of ammonium perchlorate in the propellant, and thus related to the filling process [1]. A common feature of all propellant compositions giving a bump is a high solids fraction, not less than 70% by weight (mostly ammonium perchlorate) dispersed in a binder. Unfortunately, the current understanding of a densely packed particle/fluid system is rather poor and no simple explanation is satisfactory. Furthermore, non-Newtonian behavior is expected during the filling process which makes the theoretical analysis of the practical system very difficult.

In a previous report [2], preliminary investigation was performed by using the multiple velocity field model. This is a continuum approach as opposed to a discrete particle track. It was demonstrated in the preliminary investigation that, by using different velocity boundary conditions for the two fluids, partial component separation was predicted. No slip was assumed for the liquid binder while free slip was assumed for the ammonium perchlorate particles, since particle velocity may have a finite value at the wall. Even though the results are encouraging, it was pointed out that while the multi-fluid model is more complete than the diffusion model, there are more unknown coefficients associated with the model, and these coefficients need to be determined either experimentally and/or theoretically.

In this report, the multifluid model will be adopted. Emphasis will be placed on identifying important parameters (dimensional or dimensionless) for the two-fluid model. An attempt will be made to narrow down the parameters range and to interpret the results of the multifluid model that are relevant to the solid propellant casting process.

## 2.0. IMPORTANT PARAMETERS

The momentum equations for a two-fluid system are

$$\begin{aligned} & \frac{\partial}{\partial t} (\theta_1 \rho_1 \bar{U}_1) + \nabla \cdot (\theta_1 \rho_1 \bar{U}_1 \bar{U}_1) \\ &= - \theta_1 \nabla P + \nabla \cdot \bar{\tau}_{1m} + \theta_1 \rho_1 \bar{f}_1 - K_{12} (\bar{U}_1 - \bar{U}_2) \end{aligned} \quad (1)$$

$$\begin{aligned} & \frac{\partial}{\partial t} (\theta_2 \rho_2 \bar{U}_2) + \nabla \cdot (\theta_2 \rho_2 \bar{U}_2 \bar{U}_2) \\ &= - \theta_2 \nabla P + \nabla \cdot \bar{\tau}_{2m} + \theta_2 \rho_2 \bar{f}_2 - K_{21} (\bar{U}_2 - \bar{U}_1) \end{aligned} \quad (2)$$

where  $\theta_1$ ,  $\rho_1$ ,  $\bar{U}_1$  refer to the volume fraction, the material density, and the velocity of the binder respectively, subscript 2 refers to the particles (ammonium perchlorate),  $\tau_{1m}$  is the shear stress of component 1 in the mixture,  $f_1$  is the field force per unit mass on component 1 and may include that due to shear lifting effect,  $P$  is pressure,  $K_{12}$  is the interfacial momentum transfer

coefficient between the two phases, etc. The parameters and properties needed are  $f_1$ ,  $f_2$ ,  $\tau_{1m}$ ,  $\tau_{2m}$ ,  $\theta_1$ ,  $\theta_2$ ,  $f_1$ ,  $f_2$ ,  $K_{12}$ , and  $K_{21}$ . Additional key parameters are the particle size and its distribution. The volume fractions are related,

$$\theta_1 + \theta_2 = 1 \quad (3)$$

The field forces ( $f_1$  and  $f_2$ ) will be treated separately and are not included in the present investigation. The shear stress terms ( $\tau_{1m}$  and  $\tau_{2m}$ ) are not readily determined at this time for dense suspensions. In the numerical calculations, it is simply assumed that each of the two fluids behave in a Newtonian fashion and the viscosity of each fluid is not affected by the presence of the other fluid. Even with this simplified assumption, it is still difficult to determine the viscosity of the second fluid, i.e., ammonium perchlorate particles.

The interfacial momentum transfer coefficients ( $K_{12}$  and  $K_{21}$ ) can be expressed as

$$K_{12} = \theta_1 \rho_1 F_{12} , \quad (4)$$

$$K_{21} = \theta_2 \rho_2 F_{21} , \quad (5)$$

where  $F_{12}$  is the inverse relaxation time for momentum transfer from phase 2 to phase 1, etc., and

$$K_{12} = K_{21} \quad (6)$$

from action and reaction. For the motion of a particle suspended in a fluid in the Stokes regime [3],

$$F_{21} = \frac{9\mu_1}{2a^2\rho_2} , \quad (7)$$

where  $a$  is the radius of the particle,  $\mu_1$  is the viscosity of the fluid, and  $\rho_2$  is the material density of the particle. Combining Eqs. 5, 6, and 7, the following equation is obtained:

$$\frac{K_{12} a^2}{\mu_1} = \frac{9\theta_2}{2} . \quad (8)$$

If a dimensionless interfacial momentum transfer coefficient is defined as

$$D = \frac{K_{12} a^2}{\mu_1} , \quad (9)$$

then



$$D = \frac{9 \theta_2}{2}, \quad (10)$$

which is valid only for a single particle suspended in a fluid medium in the Stoke's regime.

For a cloud of particles suspended in a fluid stream, the inverse relaxation time is [3],

$$F_{21} = \frac{75 (1 - \theta_1) \mu_1}{2 \theta_1^2 \rho_2 a^2} + \frac{1.75 \rho_1 u_s}{2 \theta_1^2 \rho_2 a} \quad (11)$$

where  $u_s$  is the superficial fluid velocity based on unobstructed flow area. In the interest of the solid propellant system, the largest particle size is in the order of  $a = 100 \mu\text{m}$ . The viscosity of the binder ( $\mu_1$ ) is relatively large ( $\sim 200 \text{ Pa-s}$  versus  $10^{-3} \text{ Pa-s}$  for room temperature water). Thus, the first term on the right-hand side is dominating for the solid propellant system. Therefore, Eq. 11 can be written

$$F_{21} \approx \frac{75 \theta_2 \mu_1}{2 \theta_1^2 \rho_2 a^2}. \quad (12)$$

Combining Eqs. 4, 5, and 12,

$$D = \frac{K_{12} a^2}{\mu_1} = \frac{75}{2} \left( \frac{\theta_2}{\theta_1} \right)^2. \quad (13)$$

Equations 10 and 13 indicate that the dimensionless interfacial momentum transfer coefficient, which is a function of volume fraction only, is the relevant scaling parameter for interfacial momentum transfer. For given volume fraction ( $\theta_1$  or  $\theta_2$ ), Eqs. 10 and 13 can be used to estimate the order of magnitude of  $D$  for single particle and a cloud of particles suspended in a fluid stream, respectively.

In addition to the dimensionless interfacial momentum transfer coefficient  $D$ , the viscosity ratio, defined as

$$Z = \frac{\mu_2}{\mu_1}, \quad (14)$$

is another important parameter since the velocity and volume fraction distributions will depend strongly on the relative magnitude of the two viscosities in the two-fluid model.

The particle size and its distribution will significantly affect the outcome of the solid propellant casting process. The two-fluid model is not capable of dealing with a system with a number of particle sizes. However, by using certain physical models, such as the Probstein-Sengun bimodal model [4],

it is possible to include the contribution from various particle sizes in a two-fluid model, and therefore avoid going to a multifluid model which will only introduce more unknowns, with current status of knowledge a fluid system with multiple particle sizes.

### 3.0. EFFECTS OF INTERFACIAL DRAG AND RELATIVE VISCOSITY

To investigate the effects of interfacial momentum transfer and relative viscosity of two fluids, steady-state calculations were performed for an annular flow, which is the two-dimensional axisymmetric flow between two concentric cylindrical surfaces employed in previous investigations [2]. The characteristics of the geometry, values of properties, and boundary conditions are given in Table 1.

Table 1. Properties and Characteristics of Annular Flow

Inner Radius, $R_i$	1.905 cm
Outer Radius, $R_o$	2.540 cm
Gap	0.635 cm
Inlet Velocity $U_1 = U_2 = U_o$	1.0 cm/s
Inlet Volume Fraction	
$\theta_1$ (binder)	0.2242
$\theta_2$ (particle)	0.7758
Material density	
$\rho_1$ (binder)	920 kg/m <sup>3</sup>
$\rho_2$ (particle)	1950 kg/m <sup>3</sup>
Velocity Boundary Condition	
Binder	no slip
Particle	free slip

An average particle size with a radius of 100  $\mu\text{m}$  is assumed. Since the average diameter (or radius) is used, the particle volume fraction can exceed the maximum packing fraction for particles with a single diameter. The binder viscosity ( $\mu_1$ ) is assumed to be equal to 200 Pa-s.

Figures 1 through 8 show the fully-developed velocity and volume fraction distributions at the exit of an annular duct for different values of the dimensionless interfacial momentum transfer coefficient  $D$ , and viscosity ratio  $Z$ . For a viscosity ratio of  $Z = 1$ , Figs. 1 through 4 indicate that the effects of interfacial parameter  $D$  begin to appear when it is decreased from 0.50 to 0.05 and the effects become appreciable when  $D = 0.005$ . Significant separation occurred when  $D = 0.005$ , as shown in Figs. 3 and 4. When the interfacial momentum transfer coefficient is large ( $D \geq 0.5$ ), there is very

little separation and the volume fraction of either the binder or the particle remains nearly constant across the duct. This is understandable since the two fluids will move as a single fluid if the interfacial drag  $D$  becomes large.

Figures 5 through 8 show the effects of viscosity ratio ( $Z = \mu_2/\mu_1$ ) on velocity and volume fraction distributions for  $D = 0.005$ . It can be observed that the viscosity ratio affects the volume fraction distribution somewhat, but the most pronounced effect appears in the particle velocity distribution as shown in Fig. 6. If the particle viscosity is much larger than the binder viscosity (for example,  $Z = 8.70$ ), then the particles move in a manner as if the binder is absent. On the other hand, if the binder viscosity is much larger than that of the particles (for example,  $Z = 0.04$ ), the particle velocity distribution becomes closer to the binder velocity distribution. The binder velocity distribution appears to be less sensitive to the viscosity ratio.

Two additional interesting phenomena were observed from the numerical results. If the interfacial momentum transfer coefficient is large ( $D > 1$ ), the volume fraction distributions for both the binder and the particles are uniform and are independent of the value of the viscosity ratio  $Z$ . This means that there is a limiting value of  $D$  ( $\approx 1$ ), above which there is no separation and below which separation does occur. This result indicates that it is extremely important to determine the value of the dimensionless interfacial momentum transfer coefficient for the solid propellant system. The authors are not aware of any existing theoretical/experimental model that can accurately predict the value of  $D$  for a densely packed system such as the solid propellant system. Further experimental and theoretical investigation in this direction will be very helpful.

The second interesting phenomenon occurs near the transition point between separation and no separation ( $D \approx 1$ ). Figures 9 and 10 show the binder and the particle volume fraction distributions for  $D = 1$  and  $Z = 10$ . At such a high value of  $D$ , separation is minute, but finite. This can be observed from the M-shaped or W-shaped profile and the small increment in the vertical scale shown in Fig. 9 or 10. The reason for the existence of an M-shaped (or W-shaped) profile is not clearly understood at this time.

#### 4.0. DISCUSSIONS

In the preliminary investigation, both the multifluid model and the single velocity field model were proposed [2]. In the multifluid model, the transport properties  $F_{12}$ ,  $\mu_m$ , etc., are not readily computed or measured. The closeness of the phase velocities suggest that the mixture velocity may be sufficiently representative. This leads to the development of a single velocity field model described in Ref. 2. It is recognized that the inverse relaxation time ( $F_{12}$ ) and the mixture viscosity  $\mu_m$  still have to be determined experimentally. However, it is difficult to visualize how a single fluid model can produce particle separation observed in the solid propellant system.

In the investigation of dense slurry rheology, Probstein and Sengun [4] recently proposed a bimodal model to describe the polymodal behavior of coal-water slurries. Their model appears to have some merit and seems relevant to the solid propellant casting process. In the bimodal model, the following definitions were employed

$$\theta_v = \frac{V_c + V_f}{V_c + V_f + V_\ell}$$

$$\theta_{ff} = \frac{V_f}{V_f + V_\ell}$$

$$\theta_c = \frac{V_c}{V_f + V_\ell + V_c}$$

where  $\theta_v$  is the volume fraction of the suspended solids,  $\theta_{ff}$  is the fine-filler volume fraction,  $\theta_c$  is the coarse particle volume fraction,  $V_f$  is the volume of the fine filler,  $V_c$  is the volume of the coarse particles, and  $V_\ell$  is the volume of the fluid. It is further defined that

$$\eta_{nr} = \eta_{cr} \cdot \eta_{fr} = \left( \frac{\mu_c}{\mu_f} \right) \left( \frac{\mu_f}{\mu_0} \right)$$

where

$\eta_{nr}$  = net relative viscosity =  $\mu_c/\mu_0$ ,

$\eta_{cr}$  = coarse relative viscosity =  $\mu_c/\mu_f$ ,

$\eta_{fr}$  = fine relative viscosity =  $\mu_f/\mu_0$ ,

$\mu_c$  = apparent viscosity of the suspension,

$\mu_f$  = apparent viscosity the suspending fluid with fine particles present, and

$\mu_0$  = viscosity of the pure liquid.

The basic assumptions in the Probstein-Sengun model are

$$\eta_{cr} = f(\theta_c)$$

and

$$\eta_{fr} = f(\theta_{ff}).$$

They further assumed that it is the small volume fraction of the colloidal size particles that imparts to the suspension most of its rheological characteristics (shear rate dependent viscosity). The large particles are essentially unaware of the presence of fine particles, but rather see a stiffened fluid that has the same viscosity and density as the suspension, with the contribution of the large particles to the viscosity increase coming about from hydrodynamic dissipation (independent of shear rate). These assumptions were supported by experimental data at low shear rate. The demarkation between fine and coarse volume fractions for six different coal/water slurries ranged from 2 to 8 microns, with an average of about 4.5 microns, even though the particle diameters in the slurries ranged from 0.5 to 300 microns. Thus, the viscosity of a polymodal system can be represented approximately by the viscosity of a bimodal system. This greatly simplifies the analysis and therefore is the more practical approach than the multifluid

model. The composition of solid propellant contains particles and powders of various sizes and is extremely difficult to handle. The bimodal model of Probstein and Sengun appears to offer a reasonable alternative. Of course, there are limitations for the application of the bimodal model as described in Ref. 4. In addition, the bimodal model does not address the problems related to particle/particle interaction, shear lift, and particle/ wall interaction.

## 5.0. SUMMARY

- (1) A two-fluid model is employed to investigate the velocity and volume fraction distributions in an annular duct. A no slip boundary condition was assumed for the fluid (the continuous phase) and free slip was assumed for the particles (the dispersed phase) at the walls. Two important dimensionless parameters were identified and parametric studies were carried out by varying these parameters. The most important parameter is the dimensionless interfacial momentum transfer coefficient  $D (= K_{12}a^2/\mu_1)$ , and the second parameter is the viscosity ratio of the two-fluid  $Z (= \mu_2/\mu_1)$ . Both parameters can affect the velocity and volume fraction distributions significantly.
- (2) Numerical results indicate that for relatively small values of  $D$ , the dimensionless interfacial momentum transfer coefficient ( $D < 0.05$ ), significant separation between the binder and the particles are observed. The smaller the  $D$ , the larger the degree of separation. Viscosity ratio  $Z$  also affects the volume fraction distribution, but its influence is somewhat less than that of the interfacial momentum transfer coefficient  $D$ .
- (3) The degree of separation decreases with increasing values of the interfacial momentum transfer coefficient. When  $D$  is sufficiently high ( $>1$ ), separation no longer exists. This is understandable since when interfacial momentum transfer is dominating, the two fluids move like a single fluid and consequently, there is very little separation. Currently, there is no theoretical or experimental model that can accurately predict the value of the interfacial momentum transfer coefficient for the solid propellant system. Further investigation, either theoretical or experimental, in this direction will be extremely helpful.
- (4) An interesting phenomenon is observed near the transition between separation and no separation ( $D \approx 1$ ). The degree of separation is rather small at  $D = 1$ , but the particle volume fraction distribution exhibited an M-shaped profile which is not present for  $D$  much smaller than 1. The reason for the existence of such an M-shaped profile is not clearly understood at this time.
- (5) The bimodal model proposed by Probstein and Sengun may be advantageous and relevant to the solid propellant system since it allows the use of a bimodal viscosity model to represent a polymodal system. This is a more practical approach than using the multifluid model since the latter will only introduce more unknowns.

- (6) It is suggested that a logical next step is to incorporate the non-Newtonian behavior of the binder into the two-velocity numerical model. This can be accomplished by modifying the present computer program to include the effects of shear-rate dependent viscosity in the following form

$$u = c \left| \frac{\partial u}{\partial r} \right|^n,$$

where  $c$  is an empirical constant,  $\frac{\partial u}{\partial r}$  is the local shear rate, and the exponent  $n$  accounts for various rheological behaviors of the fluid.

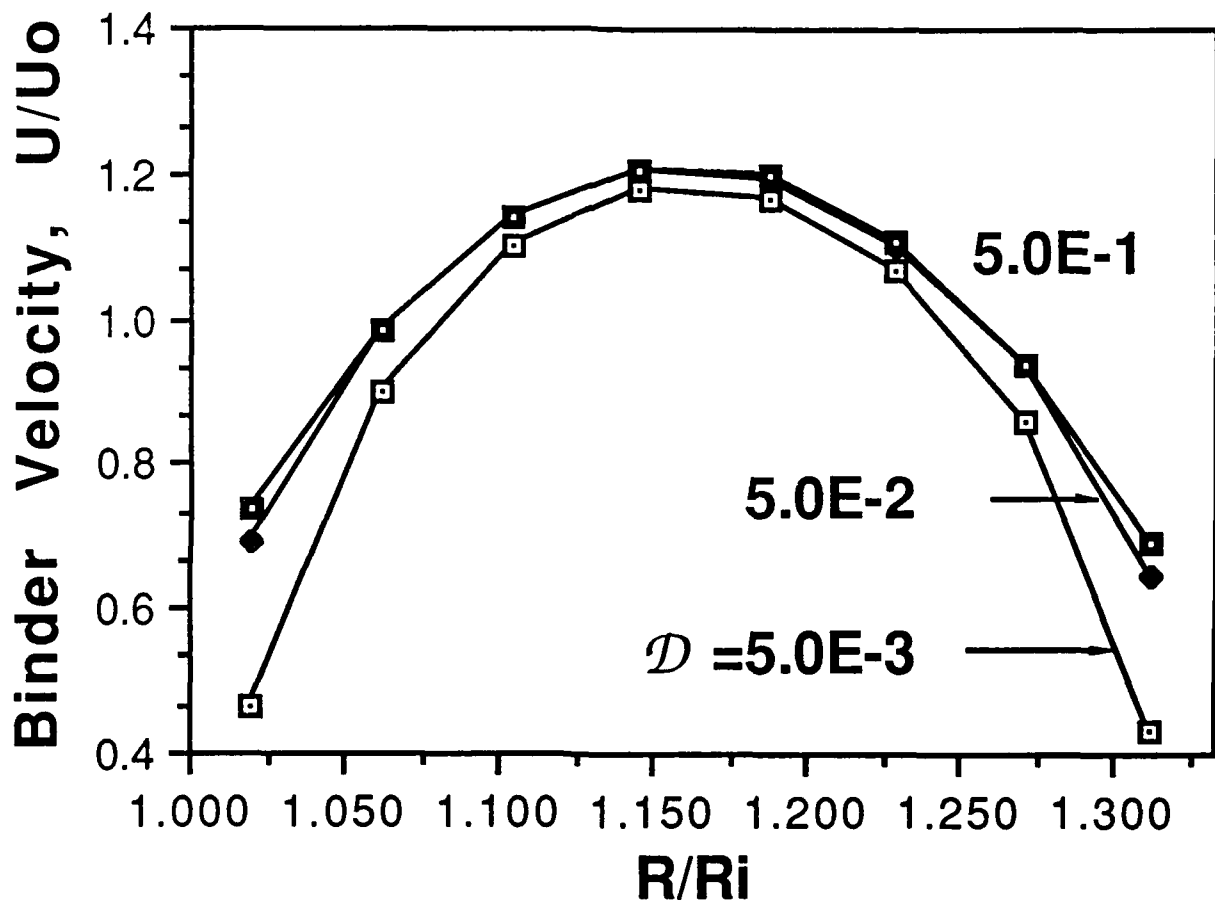


Fig. 1. Fully-Developed Velocity Distributions at the Exit of an Annular Duct ( $Z = 1$ )

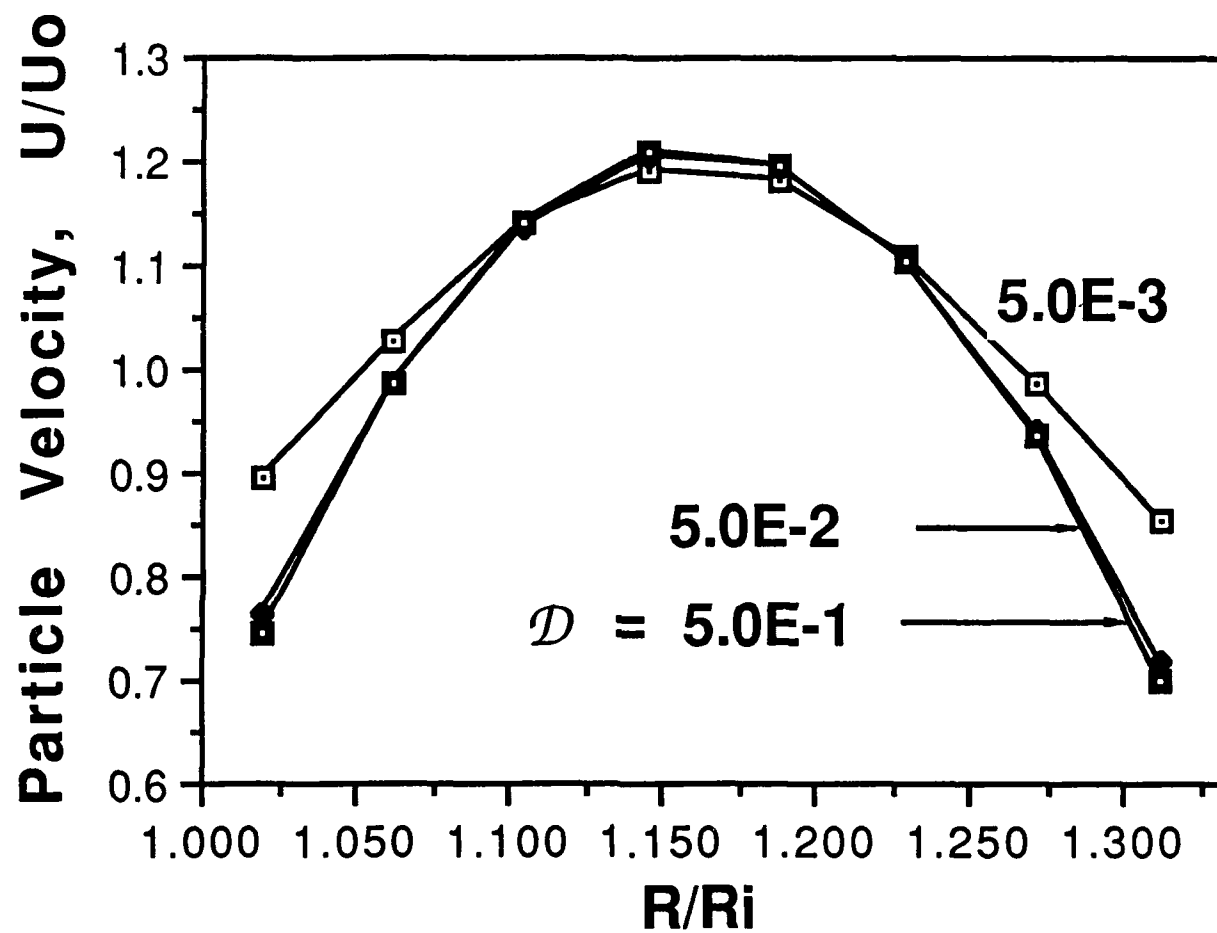


Fig. 2. Fully-Developed Particle Velocity Distribution at the Exit of an Annular Duct ( $Z = 1$ )



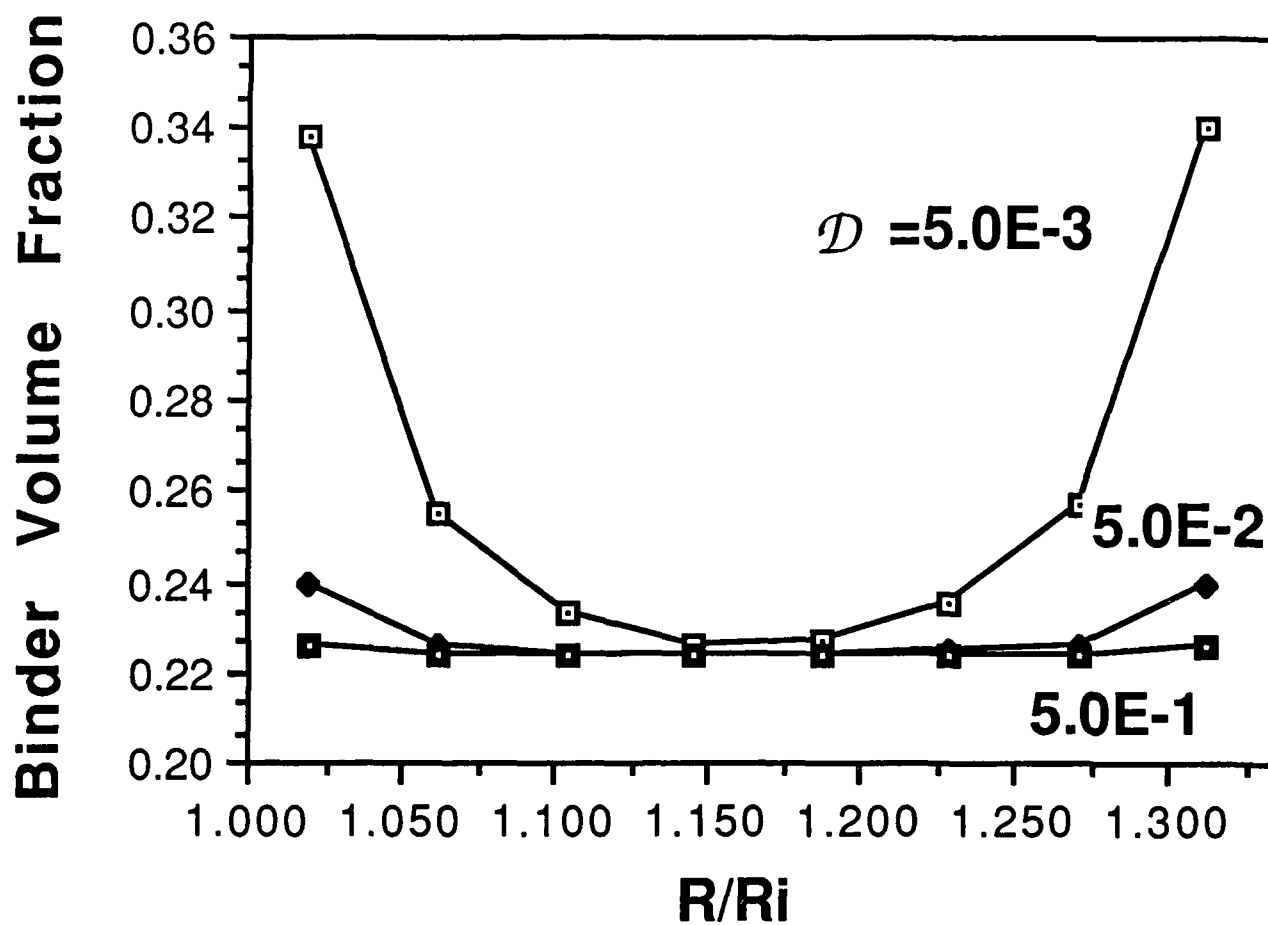


Fig. 3. Fully-Developed Binder Volume Fraction Distribution at the Exit of an Annular Duct ( $Z = 1$ )

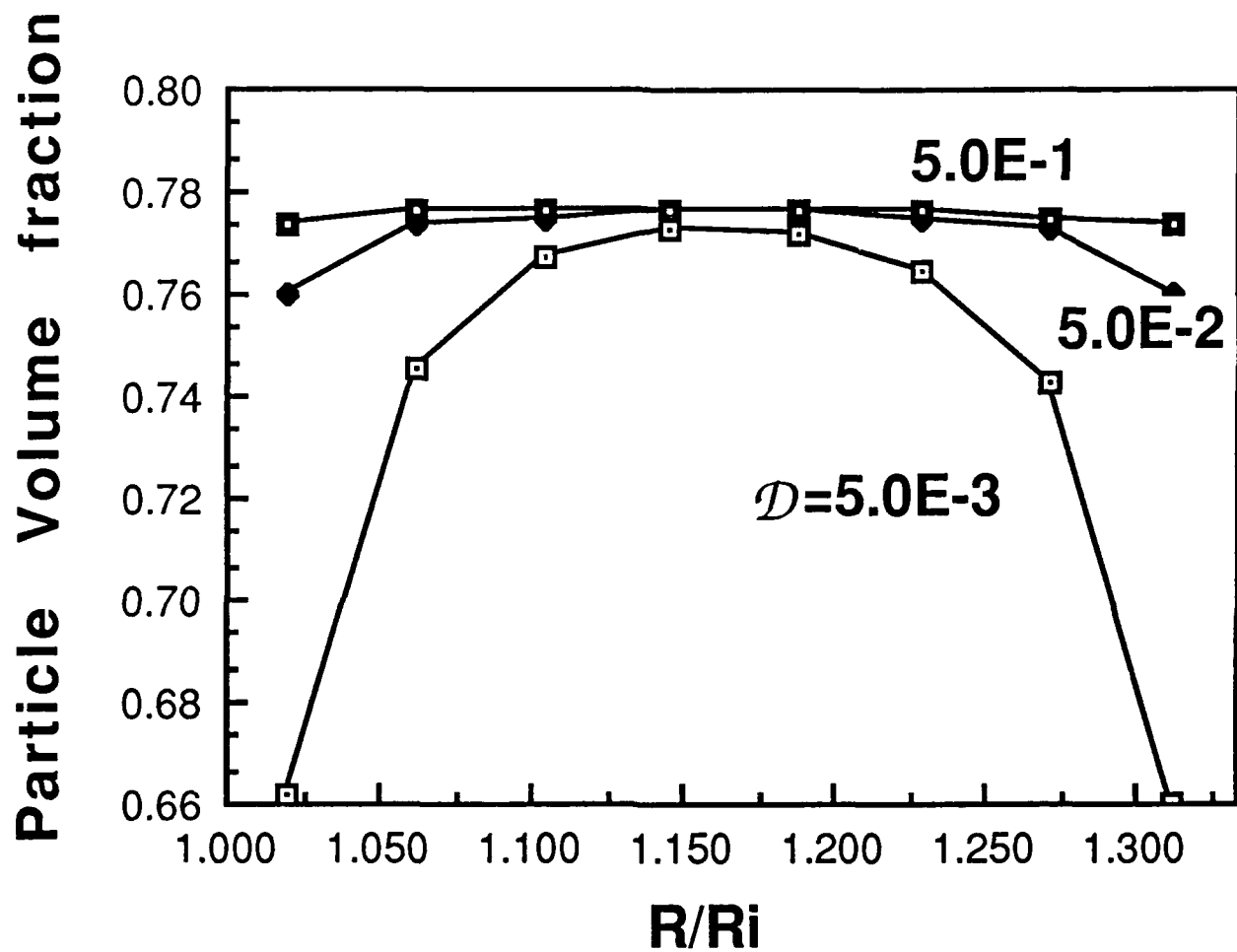


Fig. 4. Fully-Developed Particle Volume Fraction Distribution at the Exit of an Annular Duct ( $Z = 1$ )

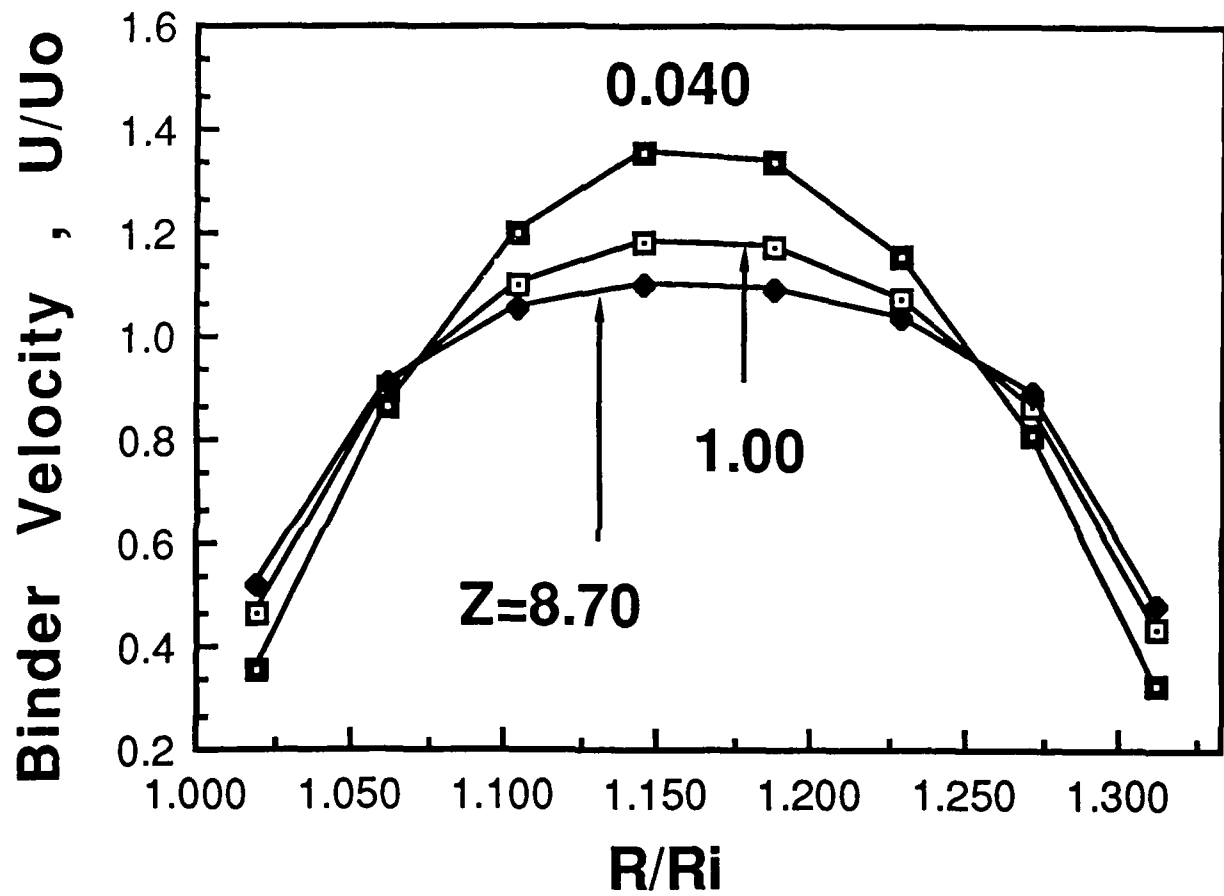


Fig. 5. Fully-Developed Binder Velocity Distribution at the Exit of an Annular Duct ( $D = 0.005$ )

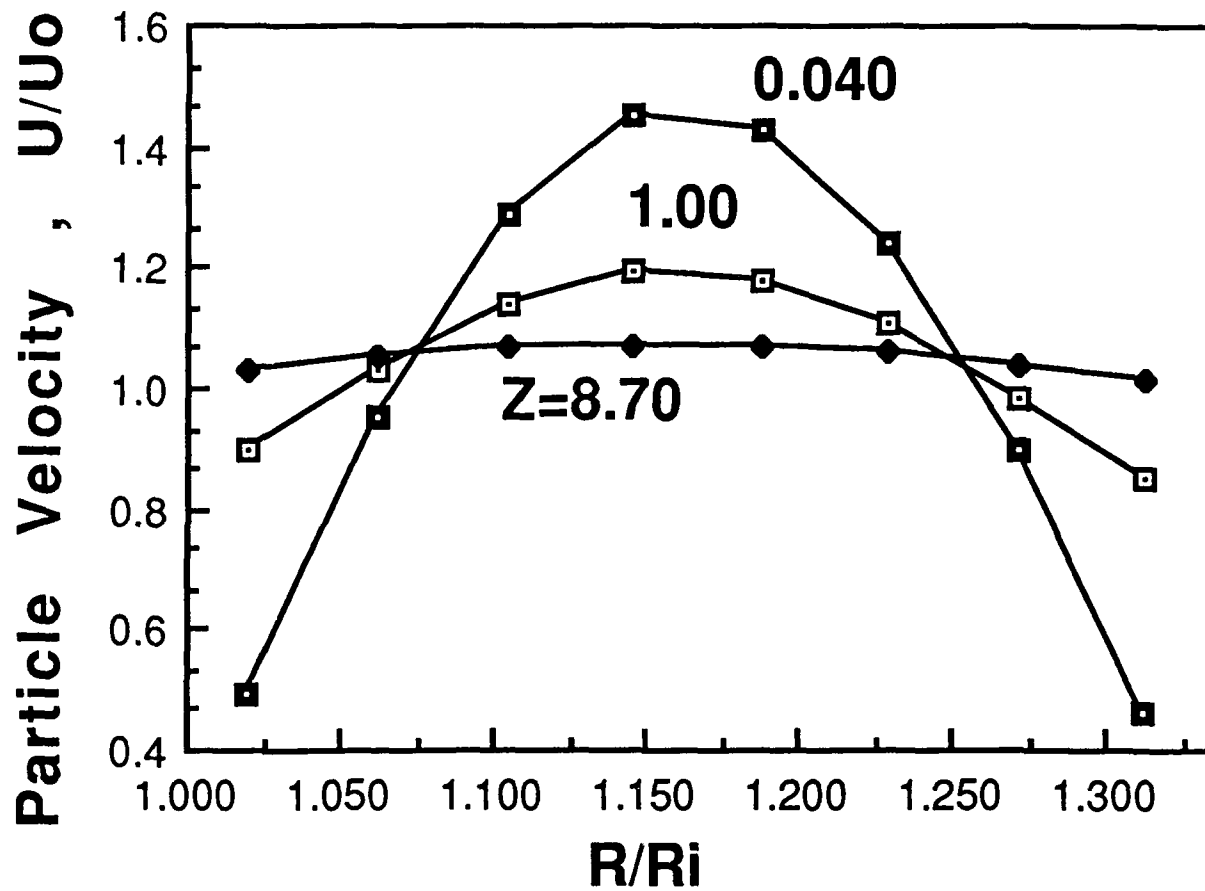


Fig. 6. Fully-Developed Particle Velocity Distribution at the Exit of an Annular Duct ( $D = 0.005$ )

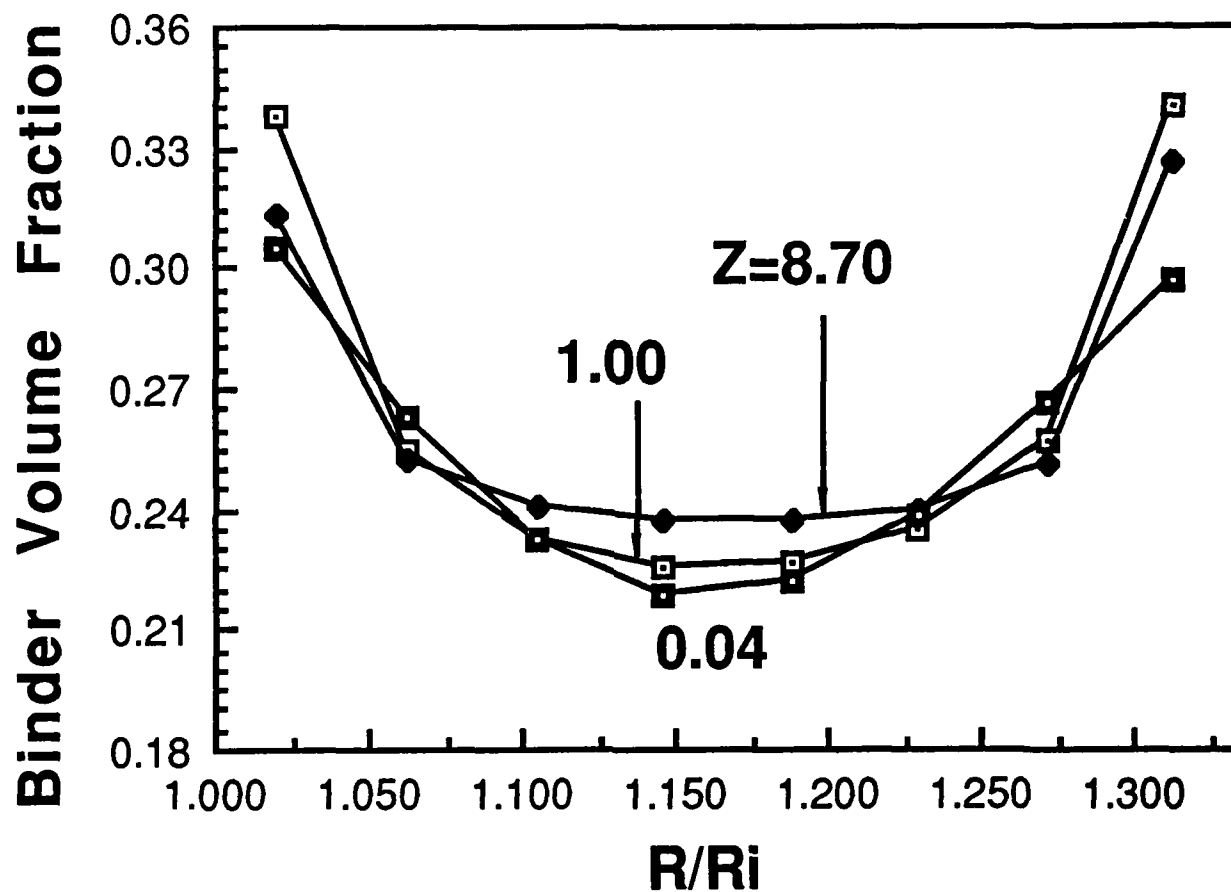


Fig. 7. Fully-Developed Binder Volume Fraction Distribution at the Exit of an Annular Duct ( $D = 0.005$ )

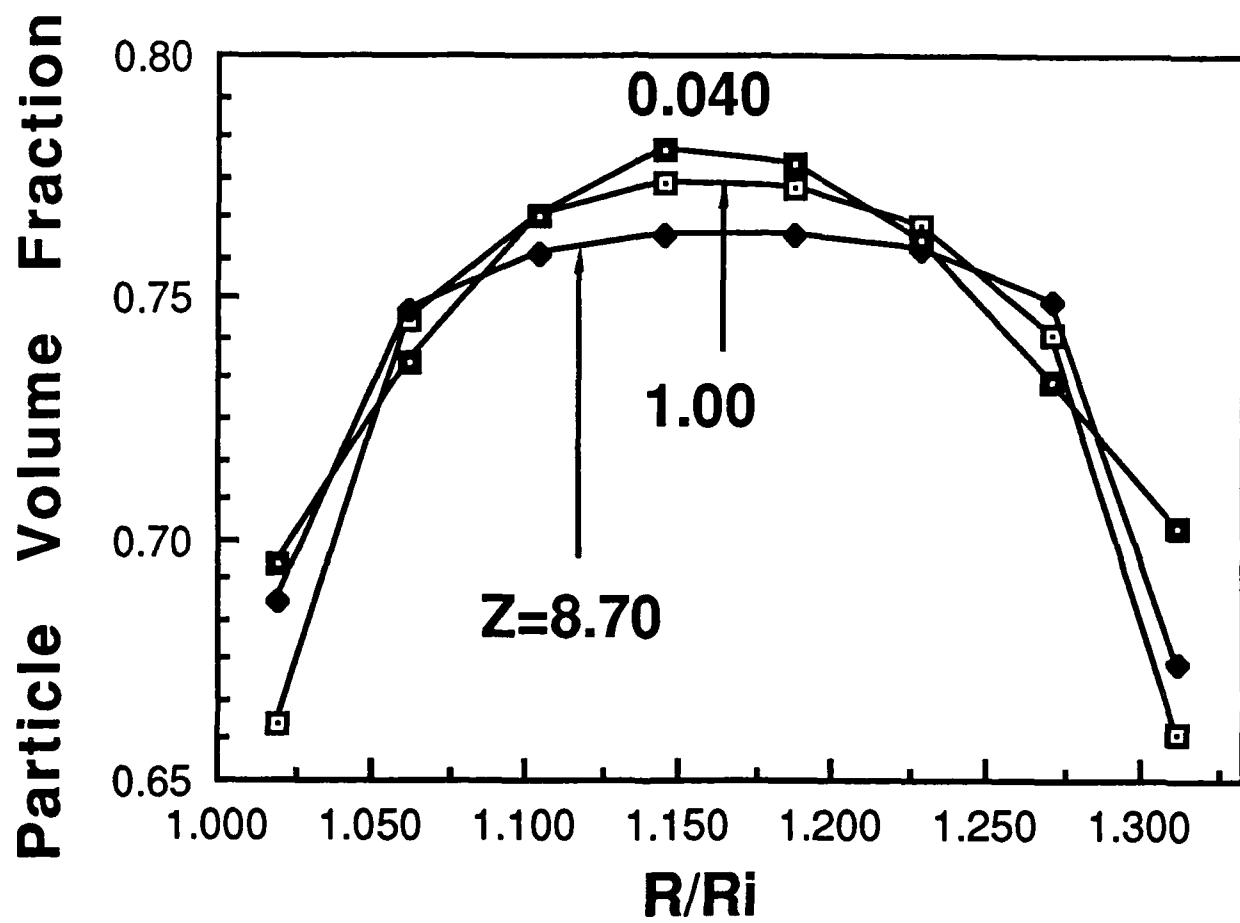


Fig. 8. Fully-Developed Particle Volume Fraction Distribution at the Exit of an Annular Duct ( $D = 0.005$ )

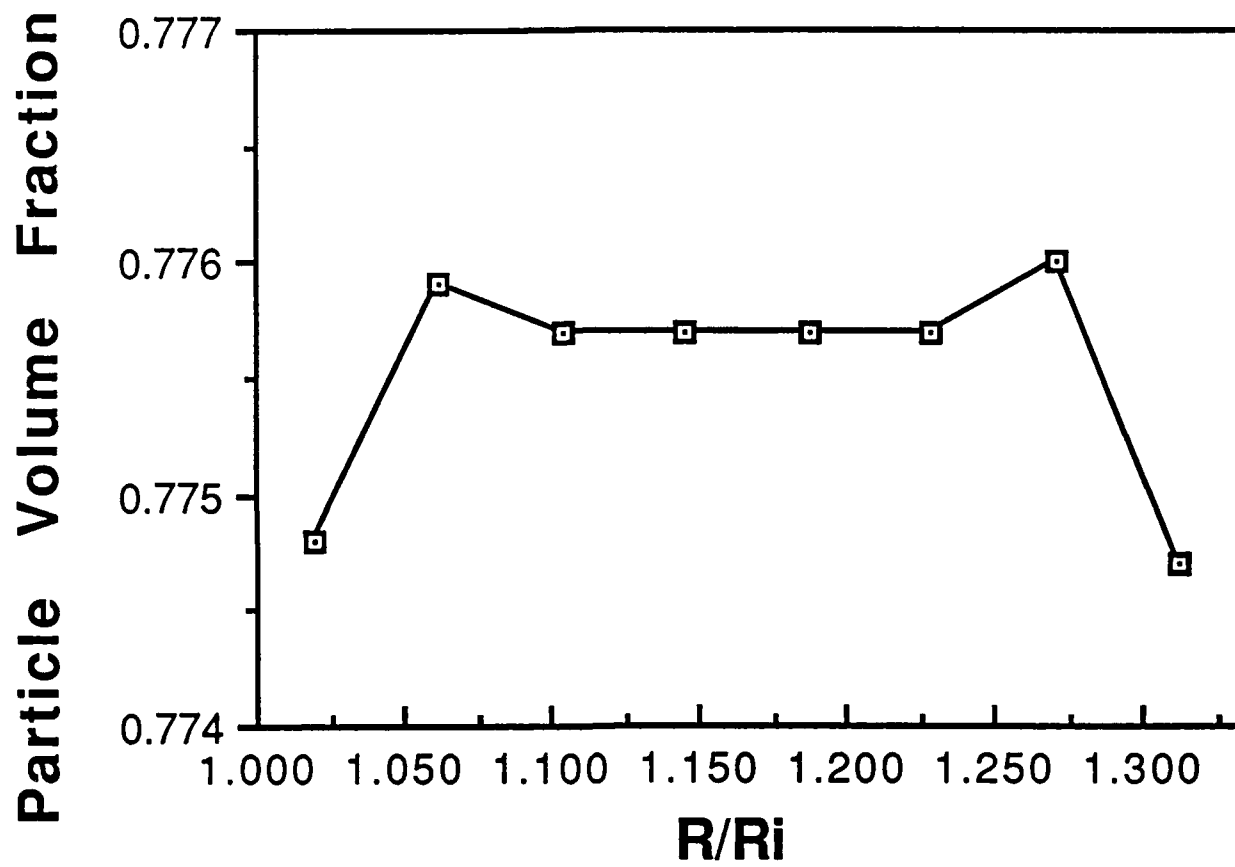


Fig. 9. Particle Volume Fraction Distribution at the Exit of an Annular Duct with  $D = 1$  and  $Z = 10$

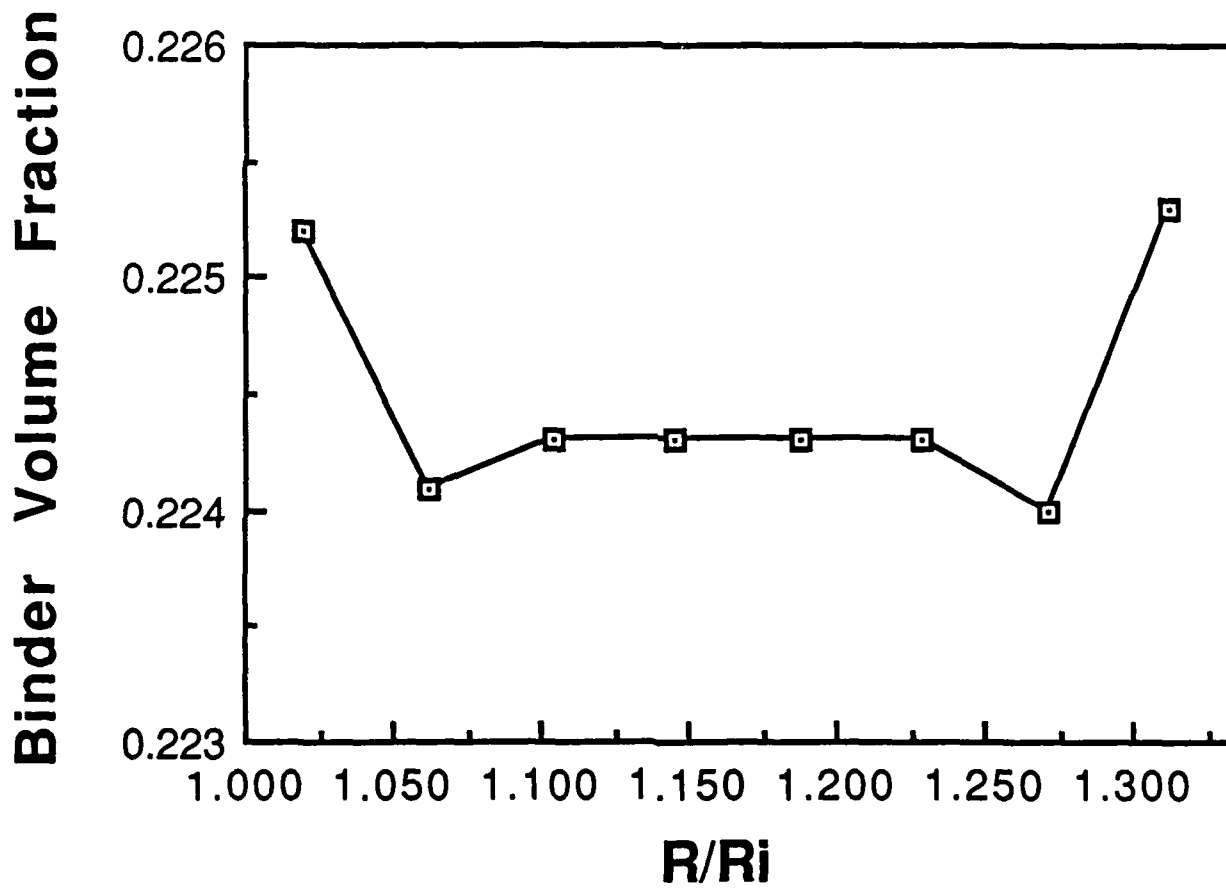


Fig. 10. Binder Volume Fraction Distribution at the Exit of an Annular Duct with  $D = 1$  and  $Z = 10$



## REFERENCES

1. W. A. Brafield, Paper No. 35C/69, T.T.C.P. Panels D5 and 03, Joint Meeting, Australia (1969).
2. H. M. Domanus, W. T. Sha, and S. L. Soo, "Preliminary Investigation of Flow Modeling During Solid Propellant Processing," Technical Report CR-RD-PR-88-1, U.S. Army Missile Command, Redstone Arsenal, Alabama, 35898-5000 (February 1988).
3. S. L. Soo, Fluid Dynamics of Multiphase Systems, Blaisdell (1967).
4. R. F. Probstein and M. Z. Sengun, "Dense Slurry Rheology with Application to Coal Slurries," Physico Chemical Hydrodynamics, Vol. 9, No. 1/2, pp. 299-313 (1987).

# DISTRIBUTION

	<u>No. of Copies</u>
Commander Naval Weapons Center Code 3272 China Lake, CA 93555-6001	1
Air Force Astronautics Laboratory AFAL/MKPA Edwards Air Force Base, CA 93523-5000	1
Director Ballistic Research Laboratory LABCOM (ATTN: AMDAR-BL) Aberdeen Proving Ground, MD 21005	1
Director U.S. Army Research Office ATTN: DRXRO-IP P.O. Box 12211 Research Triangle Park, NC 27709-2211	1
Naval Surface Weapons Center Code R11 Indian Head, MD 20640	1
Argonne National Laboratory Components Technology Division ATTN: Dr. W. T. Sha 9700 South Cass Avenue Argonne, IL 60439	10
US Army Materiel System Analysis Activity ATTN: AMXSY-MP Aberdeen Proving Ground, MD 21005	1
IIT Research Institute ATTN: GACIAC 10W. 35th Street Chicago, IL 60616	1

DISTRIBUTION (Continued)

Commander AD (XRC) ATTN: T. O'Grady Eglin AFB, FL 32542	1
Aer jet Tactical Systems ATTN: R. Mironenko P.O. Box 13400 Sacramento, CA 95813	1
Aerospace Corporation ATTN: Library Acquisition GP M1-199 P.O. Box 92957 Los Angeles, CA 90009	1
Commander AFATL ATTN: CPT Darla M. Roberts Eglin AFB, FL 32542	1
Commander AFRPL (DYP) ATTN: David P. Weaver Edwards AFB, CA 93523	1
Commander AFRPL (LK) Liquid Rocket Division ATTN: LK, Stop 24 Edwards AFB, CA 93523	1
Commander AFRPL (MKAS) ATTN: John H. Clark Edwards AFB, CA 93523	1
Commander AFRPL (Tech Lib) ATTN: Tech Lib Edwards AFB, CA 93523	1
Commander AFRPL (TSPR) ATTN: (TSPR) Stop 24 Edwards AFB, CA	1
Commander AFSC ATTN: DLFP Andrews AFB Washington, DC 20334	1

DISTRIBUTION (Continued)

Commander AFWAL (MLTN) ATTN: Charles S. Anderson Wright-Patterson AFB, OH 45433	1
Commander Armament Rsch & Dev Command ATTN: AMSMC-LC (D), (Dr. Jean-Paul Picard) Dover, NJ 07801	1
Commander Armament R&D Command ATTN: AMSMC-LCA-G(D), (Dr. Anthony J. Beardell) Dover, NJ 07801	2
Commander Armament R&D Command ATTN: AMSMC-SCA-T (D), (Mr. Ludwig Stiefel) BG 455 Dover, NJ 07801	1
Commander Armament R&D Comand Scientific & Tech Div ATTN: AMSMC-TSS(D) BG 59 Dover, NJ 07801	1
Director Army Ballistic Research Labs ATTN: AMSMC-BLA-S(A), (R. Paul Ryan) Aberdeen Proving Ground, MD 21005	1
Director Army Ballistic Research Labs ATTN: AMSMC-BLI(A), (John M. Hurban) Aberdeen Proving Ground, MD 21005	1
Director Army Ballistic Research Labs ATTN: AMSMC-BLV(A), (Richard Vitali) Aberdeen Proving Ground, MD 21005	1
Commander US Army Materiel Command ATTN: AMCDE-DW 5001 Eisenhower Ave Alexandria, VA 22333	1

DISTRIBUTION (Continued)

Commander Army Materiel System Analysis Activity ATTN: AMXSY-PS-SCTY Spec. Abdeen Proving Ground, MD 21005	1
Chief Army Research Office Information Proc Ofc ATTN: AMXRO-PP-LIB P.O. Box 12211 Research Triangle Park, NC 27709	1
Atlantic Research Corp. ATTN: Technical Info. Ctr 7511 Wellington Rd. Gainesville, VA 22065	2
California Institute of Technology Jet Propulsion Laboratory ATTN: Lib. Acqs/Standing Orders Floyd A. Anderson 4800 Oak Grove Drive Pasadena, CA 91103	1 1
Administrator Defense Technical Information Center ATTN: DTIC-DDA Cameron Station BG 5 Alexandria, VA 22314	2
Commander ESMC(PM/STINFO) ATTN: L. M. Adams Patrick AFB, FL 32925	1
FMC Corp., Northern Ord. Div ATTN: Library, (E. Schultz) 4800 East River Rd Minneapolis, MN 55421	1
Ford Aerospace & Comm. Corp. Aeronutronic Division ATTN: Tech Inf. Svc/DDC Acqs. Ford & Jamobree Roads Newport Beach, CA 92663	1
Commander FTD(TQTA) ATTN: Arnold Crowder Wright-Patterson AFB, OH 45433	1

DISTRIBUTION (Continued)

Commander  
FTD(SDBP)  
ATTN: SDBP 1  
Wright-Patterson AFG, OH 45433

Gould Defense Sys. Inc.  
Ocean Systems Div.  
ATTN: Info. Ctr, Dept. 749 PLT 2  
R. J. Rittenhouse 1  
18901 Euclid Ave.  
Cleveland, OH 44117

Hercules Inc.  
Aerospace Div, Allegany Ballistics Lab.  
ATTN: Library 1  
P.O. Box 210  
Cumberland, MD 21502

Hercules, Inc.  
Bacchus Works  
ATTN: 100-H-2-LIB (W. G. Young) 1  
P.O. Box 98  
Magna, UT 84044

Hercules, Inc.  
ATTN: Pub. Coord (D. A. Browne) 1  
P.O. Box 548  
McGregor, TX 76657

Hughes Aircraft Co.  
Electro Optical & Data Sys. Group  
ATTN: Tech Doc Ctr, BG E1E110)  
B. W. Campbell 1  
P.O. Box 902  
El Segundo, CA 90245

Johns Hopkins University  
Applied Physics Lab, Chem. Prop. Inf. Agy.  
ATTN: Code ML, R. D. Brown 2  
Johns Hopkins Road  
Laurel, MD 20707

LTV Aerospace & Def. Co.  
ATTN LIB 2-58010 1  
P.O. Box 225907  
Dallas, TX 75265

Marquardt Company  
ATTN: LIB 1  
P.O. Box 2013  
Van Nuys, CA 91409

DISTRIBUTION (Continued)

Martin Marietta Corp. ATTN: MP-30-TIC P.O. Box 5837 Orlando, FL 32855	1
National Aeronautics & Space Admin. George C. Marshall Space Flt Ctr. ATTN: AS24L Marshall Space Flight Center, AL 35812	1
National Aeronautics & Space Admin. George C. Marshall Space Flight Center ATTN: EP-25, Mr. John Q., Miller Marshall Space Flight Center, AL 35812	1
National Aeronautics & Space Admin Langley Research Center ATTN: MS-185 Tech. Lib. Hampton, VA 23665	1
National Aeronautics & Space Admin. Lewis Research Center ATTN: Lib(D. Morris) 21000 Brookpark Rd. Cleveland, OH 44135	1
National Aeronautics & Space Admin. Lewis Research Center ATTN: MS-501-5, D. A. Petrash 21000 Brookpark Rd. Cleveland, OH 44135	1
National Aeronautics & Space Admin. Lyndon B. Johnson Space Center ATTN: JM2/Tech. Lib. Houston, TX 77058	1
National Aeronautics & Space Admin. Scientific Technical Info. Fac. ATTN: Accessioning Dept. P.O. Box 8757 Baltimore Washington Intl Airport, MD 21240	1
Commander Naval Air Dev. Ctr. ATTN: Code 8131 Warminster, PA 18974	1
Commander Naval Air Sys. Comd. ATTN: NAIR-00D4-Tech Lib. Washington, DC 20361	1

DISTRIBUTION (Continued)

Commander  
Naval Air Sys Comd  
ATTN: NAIR-320G, Mr. Bertram P. Sobers 1  
Washington, DC 20361

Commander Officer  
Naval Intel Spt Ctr  
Information Svc Div  
ATTN: Doc Lib 1  
4301 Suitland Rd.  
Washington, DC 20390

Commanding Officer  
Naval Ord Sta-Indian Head  
ATTN: Tech Lib, Code 4243C, Henrietta Gross 1  
Indian Head, MD 20640

Superintendent  
Naval Postgraduate Sch.  
ATTN: Code 1424-Libs Dir 1  
Monterey, CA 93943

Chief Naval Research  
ATTN: Dr. Richard S. Miller, Code 432 1  
Arlington, VA 22217

Chief  
Naval Research  
ATTN: R. Junker, Code 412 1  
Arlington, VA 22217

Commanding Officer  
Naval Research Lab  
ATTN: Code 6100 1  
Washington, DC 20375

Director  
Naval Arsearch West Pasadena  
ATTN: R. J. Marcus 1  
1030 E Green St  
Pasadena, CA 91106

Commander  
Naval Sea Sys Comd  
ATTN: SEA-09B312, Tech Lib 1  
Natl Ctr BG 3  
Washington, DC 20362

Commander  
Naval Sea Sys Comd  
ATTN: Mr. Elgin Werback, SEA-62Z31B 1  
Natl Ctr BG 3  
Washington, DC 20362



DISTRIBUTION (Continued)

Commander Naval Surface Wpns Ctr ATTN: Acquisitions, Code E431 Dahlgren, VA 22448	1
Commander Naval Surface Wpns Ctr ATTN: Code E432, S. Happel, Room 1-321 Silver Spring, MD 20910	2
Commanding Officer Naval Underwater Sys Ctr ATTN: Tech Lib 021312 Newport, RI 02840	1
Commander Naval Weapon Center ATTN: Code 343 China Lake, Ca 93555	2
Director Navy Strat Sys Proj Ofc ATTN: Tech Lib Br Hd Washington, DC 20376	1
Commander Ogden ALC (MANPA) ATTN: Mr. Anthony J. Inverso BG 1941 Hill AFB, UT 84056	1
Commander Radford Army Ammo Plant ATTN: SMCRA-QA Radford, VA 24141	1
Rockwell Int'l Corp. Rocketdyne Div ATTN: Tech Info Ctr 6633 Canoga Ave Canoga Park, CA 91304	1
Rohm & Haas Co. ATTN: Scty Off, (Dr. H. M. Shuey) 723-A Arcadia Circle Huntsville, AL 35801	
Commander SAALC (SFTT) ATTN: W. E. Vandeventer Kelly AFB, TX 78241	1

DISTRIBUTION (Continued)

SRI Int'l Document Ctr ATTN: Classified Doc Svc, (Dr. Clifford D. Bedford) 333 Ravenswood Ave Menlo Park, CA 94025	1
Talley Industries ATTN: Eng. Tech Lib, (Kim St. Clair) P.O. Box 849 Mesa, AZ 85201	1
Teledyne Ryan Aeronautical ATTN: Tech Info Svcs (W. E. Ebner) 2701 Harbor Drive San Diego, CA 92101	1
Thiokol Chem Corp Wasatch Div ATTN: Tech Lib (J. E. Hansen) Brigham City, UT 84302	2
Thiokol Corp. ATTN: Scty Off, (D. J. McDaniel) P.O. Box 241 Elkton, MD 21921	1
Thiokol Corp. ATTN: Tech Lib (H. H. Sellers) Huntsville, AL 35807	1
TRW Inc. Electronics & Defense Sector ATTN: Tech Inf Ctr, Doc Svcs for S/1930 One Space Park Redondo Beach, CA 90278	2
TRW Inc. Electronics & Defense Sector ATTN: Tech Inf Ctr, Doc Svcs for R. C. Reeve, San Bernardino One Space Park Redondo Beach, CA 90278	1
USDRE (PCA) ATTN: OUSDRE&E (R&AT/MST), (Dr. Robert J. Heaston) The Pentagon, Room 3D1089 Washington, DC 20301	1
United Technologies Corp Chemical Systems Div ATTN: Tech Lib P.O. Box 358 Sunnyvale, CA 94088	1

# DISTRIBUTION (Concluded)

United Technologies Corp. Research Center ATTN: Acq Lib (M. E. Donelly) 400 Main Street East Hartford, CT 06108	1
Commander White Sands Missile Range ATTN: Tech Lib White Sands Missile Range, NM 88002	1
AMSMI-RD, Dr. McCorkle	1
Dr. Rhoades	1
Dr. Stephens	1
-RD-RE, Dr. Bennett	1
-RD-PR, Dr. Wharton	1
-RD-PR-T, Dr. Alley	1
Ms. Ducote	1
-RD-PR-P, Mr. Schultz	1
-RD-PR-M, Mr. Ifshin	1
-RD-PR-E, Mr. Maykut	5
-RD-CS-R	15
-RD-CS-T	1
AMSMI-GC, IP, Mr. Bush	1